

# Rayleigh-wave ellipticity in weakly heterogeneous layered media

Matthew M. Haney<sup>1</sup> and Victor C. Tsai<sup>2</sup>

<sup>1</sup>*U.S. Geological Survey, Alaska Volcano Observatory, Anchorage, AK 99508-4667, USA*

<sup>2</sup>*Department of Earth, Environmental and Planetary Sciences, Brown University, Providence, RI 02912, USA. Email: [mhaney@usgs.gov](mailto:mhaney@usgs.gov)*

Received 2021 September 22; in original form 2021 May 23

## SUMMARY

We derive approximate expressions for the ellipticity (i.e. horizontal-to-vertical or vertical-to-horizontal ratio) of Rayleigh waves propagating in a layered medium. The approximation is based on the generalized energy equation for Rayleigh waves, which has been used previously to obtain perturbational results for ellipticity. For a medium with weakly heterogeneous layers, we obtain an approximation from the perturbational result by taking the background medium to be homogeneous. The generalized energy equation also requires an auxiliary function and we discuss how the various possible functions are related to the homogeneous Rayleigh-wave eigenfunction. The analysis reveals that, within the weak approximation, the product of ellipticity and squared phase velocity is linearly related to squared shear wave velocity in the subsurface. We show the accuracy of the approximation with a simple layer-over-half-space model and then demonstrate its utility in a linear inversion scheme for shear wave velocity.

**Key words:** Surface waves and free oscillations; Theoretical seismology; Wave propagation; Crustal structure.

## 1 INTRODUCTION

The mapping of Earth structure in depth with surface waves commonly uses phase or group velocities measured over a range of frequencies. Less commonly used, but still able to constrain structure, is the measurement of Rayleigh-wave ellipticity as a function of frequency (Boore & Toksöz 1969). Rayleigh-wave ellipticity is the aspect ratio of the particle motion ellipse and can be expressed as either the vertical-to-horizontal (V/H) ratio or its inverse, the horizontal-to-vertical (H/V) ratio. Within the field of engineering seismology, ellipticity information has been successfully used to constrain structure within the upper hundreds of metres of the subsurface (Fäh *et al.* 2001, 2003; Malischewsky & Scherbaum 2004; Hobiger *et al.* 2013; Chieppa *et al.* 2020). At the crustal scale, joint inversions of ellipticity derived from ambient noise together with phase velocity measurements have been shown to better resolve shallow structure (Chong *et al.* 2014; Lin *et al.* 2014; Muir & Tsai 2017; Berg *et al.* 2018) relative to the wavelength compared to inversions based on phase velocity alone. Initial results on the sensitivity of ellipticity measurements to structural parameters were obtained for a layered medium by Tsuboi & Saito (1983) and Tanimoto & Tsuboi (2009). More recent work by Maupin (2017) has addressed ellipticity sensitivity in a 3-D sense for finite-frequency data, although questions remain on the agreement between 1-D and 3-D sensitivity kernels.

The generalized energy equation for Rayleigh waves has been described by Ben-Menahem & Singh (1981) and subsequently been used by Tsuboi & Saito (1983) and Tanimoto & Tsuboi (2009) to find analytical expressions for the sensitivity kernels of Rayleigh-wave particle motion in a layered medium. Here we show how these results can be used to find approximate expressions for ellipticity in weakly heterogeneous layered media, by which we mean a subsurface layered model where the properties of adjacent layers do not vary greatly. Such approximations lead to non-perturbational inversion formulae that relate surface wave observables and subsurface shear wave velocities directly, instead of their perturbations. These non-perturbational formulae offer a method for defining a good initial model directly from data that can be subsequently refined with perturbational inversion. Haney & Tsai (2015, 2017) have previously shown such non-perturbational approaches for inverting phase velocities and made the connection to Dix inversion within the field of reflection seismology (Dix 1955). The approximate formulae for ellipticity developed here similarly lend themselves to non-perturbational inversion schemes.

## 2 BACKGROUND AND AUXILIARY FUNCTIONS

We first review the formalism of Tanimoto & Tsuboi (2009) and give the basic relations for the Rayleigh-wave eigenfunctions and also auxiliary functions we use to analyse ellipticity.

In terms of the Rayleigh-wave eigenfunctions  $y_1$  and  $y_3$ , the radial horizontal and vertical displacements are given as

$$u_x = -iy_3(z)Ue^{i(\omega t - kx)}, \quad (1)$$

$$u_z = y_1(z)Ue^{i(\omega t - kx)}, \quad (2)$$

with  $\omega$  and  $k$  the angular frequency and wavenumber, respectively, and  $U$  a dimensioned constant with physical units of displacement. Therefore,  $y_1$  and  $y_3$  are dimensionless. Similarly, the two relevant stresses for Rayleigh waves are given in terms of the Rayleigh-wave eigenfunctions  $y_2$  and  $y_4$  as

$$\sigma_{zz} = y_2(z)Ue^{i(\omega t - kx)}, \quad (3)$$

$$\sigma_{zx} = -iy_4(z)Ue^{i(\omega t - kx)}. \quad (4)$$

Due to the same dimensioned constant  $U$  appearing these expressions,  $y_2$  and  $y_4$  have the physical dimensions of pressure divided by displacement ( $\text{Pa m}^{-1}$ ). The eigenfunctions represented by  $y_1, y_2, y_3$  and  $y_4$  comprise the motion-stress vector and the components are related to each other by the following system of equations (Tanimoto & Tsuboi 2009):

$$\frac{dy_1}{dz} = \frac{1}{\lambda + 2\mu}(y_2 + k\lambda y_3), \quad (5)$$

$$\frac{dy_2}{dz} = -\rho\omega^2 y_1 + ky_4, \quad (6)$$

$$\frac{dy_3}{dz} = -ky_1 + \frac{1}{\mu}y_4, \quad (7)$$

$$\frac{dy_4}{dz} = -\frac{k\lambda}{\lambda + 2\mu}y_2 + \left[ k^2 \left( \lambda + 2\mu - \frac{\lambda^2}{\lambda + 2\mu} \right) - \rho\omega^2 \right] y_3, \quad (8)$$

where  $\mu$  is the shear modulus,  $\lambda$  is Lamé's first parameter and  $\rho$  is the density.

The V/H ratio at the free surface is given as

$$\epsilon(0) = \frac{y_1(0)}{y_3(0)}, \quad (9)$$

where the free surface is located at  $z = 0$ . We use the same notation as Tanimoto & Tsuboi (2009); in particular, we adopt a coordinate system in which the  $z$ -axis is positive upwards. However, we take the free surface to be at  $z = 0$  instead of  $z = H$  as in Tanimoto & Tsuboi (2009). The H/V ratio at the free surface is given as the reciprocal of the V/H ratio:

$$\gamma(0) = \frac{1}{\epsilon(0)} = \frac{y_3(0)}{y_1(0)}. \quad (10)$$

Most studies focus on the ellipticity at the free surface since that is where measurements are commonly made; however, ellipticity varies with depth and can in principle be measured at any depth (Meyers *et al.* 2019).

For a homogeneous medium with  $\lambda = \mu$  (Poisson medium), the  $y_1$  and  $y_3$  eigenfunctions are well known (Ewing *et al.* 1957):

$$y_3(z) = e^{0.8475kz} - 0.5773e^{0.3933kz}, \quad (11)$$

$$y_1(z) = 0.8475e^{0.8475kz} - 1.4679e^{0.3933kz}. \quad (12)$$

Note that the signs of the exponentials are positive since as mentioned previously the  $z$ -axis is directed positive upwards as in Tanimoto & Tsuboi (2009). Also, since these are eigenfunctions, they can be multiplied by an arbitrary constant. In this work, we focus on the case of a Poisson medium (one with Poisson's ratio equal to 0.25) and derive an approximate formula for ellipticity. However, the approximation can be derived for other assumed values of Poisson's ratio and we show this more detailed derivation in the Appendix. Similarly, Haney & Tsai (2015) showed approximations for phase velocity for a Poisson medium but then subsequently published the phase velocity approximations for any value of Poisson's ratio (Haney & Tsai 2017).

Eqs (11) and (12) are the solution of the system of eqs (5)–(8) subject to the boundary condition of a stress-free surface at  $z = 0$ , such that  $y_2(0) = y_4(0) = 0$ . This can be verified by computing  $y_2(z)$  and  $y_4(z)$  from  $y_1(z)$  and  $y_3(z)$  using eqs (5) and (7) and  $\lambda = \mu$ , which gives

$$y_2(z) = 1.1547k\mu \times (e^{0.8475kz} - e^{0.3933kz}), \quad (13)$$

$$y_4(z) = 1.6950k\mu \times (e^{0.8475kz} - e^{0.3933kz}). \quad (14)$$

As can be seen from these equations,  $y_2(0)$  and  $y_4(0)$  are both identically zero.

However, there are other solutions of eqs (5)–(8) that do not satisfy the stress-free boundary condition at  $z = 0$ . Among these, an important type discussed by Tanimoto & Tsuboi (2009) are called auxiliary functions. We denote these other solutions  $x_1, x_2, x_3$  and  $x_4$ , in contrast to the eigenfunctions  $y_1, y_2, y_3$  and  $y_4$  that must also satisfy the boundary conditions. There are many possible sets of  $x_1, x_2, x_3$  and

$x_4$  and they correspond to different boundary conditions. Tanimoto & Tsuboi (2009) show that the auxiliary functions and eigenfunctions are related by

$$\begin{aligned} &: \\ &\frac{d}{dz}(x_1y_2 + x_3y_4) = \\ &3\mu(\dot{x}_1 - kx_3)(\dot{y}_1 - ky_3) + \mu(\dot{x}_3 + kx_1)(\dot{y}_3 + ky_1) + 2k\mu(\dot{x}_1y_3 + \dot{y}_1x_3) - \rho\omega^2(x_1y_1 + x_3y_3) \\ &= F(\mathbf{x}, \mathbf{y}, \rho, \mu, \omega), \end{aligned} \quad (15)$$

where we have shown the relation for the case of a Poisson medium ( $\lambda = \mu$ ). As pointed out by Tanimoto & Tsuboi (2009), eq. (15) actually applies for any two solutions of eqs (5)–(8), irrespective of the boundary conditions. Integrating eq. (15) from  $-\infty$  to 0 gives

$$x_1(0)y_2(0) + x_3(0)y_4(0) = \int_{-\infty}^0 F(\mathbf{x}, \mathbf{y}, \rho, \mu, \omega)dz, \quad (16)$$

where the terms on the left-hand side evaluated at  $z = -\infty$  vanish. These terms are equal to zero since  $y_2$  and  $y_4$  approach zero at  $z = -\infty$  and we require the auxiliary functions to also approach zero at  $z = -\infty$ . Tanimoto & Tsuboi (2009) refer to this as the regularity condition for the eigenfunctions and auxiliary functions. In addition,  $y_2$  and  $y_4$  are zero at  $z = 0$  and therefore

$$x_1(0)y_2(0) + x_3(0)y_4(0) = 0, \quad (17)$$

which also means that the integral of  $F$  in eq. (16) is equal to zero as well. Furthermore, Tanimoto & Tsuboi (2009) point out that the function  $F$  is symmetric in terms of the eigenfunction vector  $\mathbf{y}$  and auxiliary function vector  $\mathbf{x}$ , that is  $F(\mathbf{x}, \mathbf{y}) = F(\mathbf{y}, \mathbf{x})$  as seen in eq. (15). Thus, by eq. (16), eq. (17) can be rewritten by exchanging  $\mathbf{x}$  and  $\mathbf{y}$ , giving

$$y_1(0)x_2(0) + y_3(0)x_4(0) = 0. \quad (18)$$

This equation can be reorganized in terms of the V/H ratio at the surface  $\epsilon(0)$ :

$$\frac{x_4(0)}{x_2(0)} = -\frac{y_1(0)}{y_3(0)} = -\epsilon(0), \quad (19)$$

which means that the ratio of the auxiliary functions related to stress at the surface is the negative of the V/H ratio of the eigenfunctions at the surface.

Here, we show the family of such functions that can be taken as the auxiliary functions. Two independent solutions of eqs (5)–(8) for a homogeneous medium are evanescent  $P$  and  $S$  waves. The Rayleigh wave for a homogeneous medium is simply a linear combination of those two solutions such that the sum satisfies the stress-free boundary conditions at  $z = 0$ . By multiplying the two terms in eqs (11) and (12) by numerical factors  $n_1$  and  $n_2$ , we arrive at these possible auxiliary functions:

$$x_3(z) = n_1 e^{0.8475kz} - 0.5773n_2 e^{0.3933kz}, \quad (20)$$

$$x_1(z) = 0.8475n_1 e^{0.8475kz} - 1.4679n_2 e^{0.3933kz}, \quad (21)$$

where  $(n_1, n_2)$  can be equal to any numbers except those for which  $n_1 = n_2$ . This restriction on  $(n_1, n_2)$  means the auxiliary functions cannot be equal to eigenfunctions. For subsequent derivations, we need to compute  $x_2$  and  $x_4$  from eqs (20) and (21), again under the assumption of a Poisson medium. This gives similar expressions to eqs (13) and (14):

$$x_2(z) = 1.1547k\mu \times (n_1 e^{0.8475kz} - n_2 e^{0.3933kz}), \quad (22)$$

$$x_4(z) = 1.6950k\mu \times (n_1 e^{0.8475kz} - n_2 e^{0.3933kz}). \quad (23)$$

At the surface  $z = 0$ , it can be easily seen that  $x_4(0)/x_2(0) = 1.4679$ . This is the negative of the V/H ratio  $y_1(0)/y_3(0)$  computed from eqs (11) and (12) to within the significant digits shown here. The equivalence can be shown to be exact if the preceding derivation had left Poisson's ratio as a variable rather than fixing it to be 0.25, but the expressions would have been unnecessarily more complex to accommodate variable Poisson's ratio.

Eq. (20) and (21) represent a family of possible choices for the auxiliary functions; we can choose any of them, for particular values of  $n_1$  and  $n_2$ , and those would be suitable choice for the auxiliary functions so long as  $n_1 \neq n_2$ . This is the inherent non-unique nature of the auxiliary functions as discussed by Tsuboi & Saito (1983) and Tanimoto & Tsuboi (2009).

### 3 VARIATIONAL RESULTS

With the auxiliary functions in eqs (20) and (21), we now review the results from the variational principle for ellipticity presented by Tanimoto & Tsuboi (2009) and show how these lead to closed-form approximations for ellipticity in weakly heterogeneous layered media. We continue to only consider a Poisson medium. In addition, the approximations we derive are for small changes in shear modulus in a medium with constant density. We do this since fundamental-mode Rayleigh waves are typically inverted for a shear wave velocity model.

Density variations have in some cases been obtained from Rayleigh-wave ellipticity (Lin *et al.* 2014), but as a first step we will only consider shear wave velocity or shear modulus variations with constant density. This also allows us to compare the approximations with the recently derived Dix approximation for Rayleigh waves (Haney & Tsai 2015, 2017; Haney *et al.* 2020), which took density as constant or known and showed that there is a linear relation between squared phase or group velocity and squared shear wave velocity in the subsurface. Such a relation between squared values of velocity measurements and squared values of subsurface velocity is equivalent to the Dix relation (Dix 1955) widely used in reflection seismology (Haney & Tsai 2015). In fact, Haney *et al.* (2020) point out that a Dix-type approximation for Rayleigh waves had been derived as early as 1935 by Sir Harold Jeffreys (Jeffreys 1935); however, the connection to the analogous expression in reflection seismology could not be made at the time since it would not appear for another 20 yr (Dix 1955).

For a perturbation in the eigenfunctions, Tanimoto & Tsuboi (2009) show in their eq. (21) that

$$\delta y_1(0)x_2(0) + \delta y_3(0)x_4(0) = -\delta k \int_{-\infty}^0 \frac{\partial F(\mathbf{x}, \mathbf{y})}{\partial k} dz - \int_{-\infty}^0 \frac{\partial F(\mathbf{x}, \mathbf{y})}{\partial \mu} \delta \mu dz, \quad (24)$$

where we suppress the dependence of  $F$  on  $\rho$ ,  $\mu$  and  $\omega$  for simplicity but it is implied. Note that we do not consider boundary perturbations (i.e. changes in the layer interface depths) as done in Tanimoto & Tsuboi (2009). Also, eq. (24) only includes perturbations in the shear modulus for a Poisson medium ( $\lambda = \mu$ ) since density is taken to be constant. We now seek to relate the left-hand side of eq. (24) to ellipticity. First we note the following perturbational result valid to first order (Tanimoto & Alvizuri 2006):

$$\frac{\delta \epsilon}{\epsilon} = \frac{\delta y_1}{y_1} - \frac{\delta y_3}{y_3}, \quad (25)$$

where the denominators are the values in the background medium and the numerators are the values in the perturbed medium minus the values in the background medium. Evaluating this at  $z = 0$  and using eq. (18) to substitute for  $y_3(0)$  we arrive at

$$y_1(0)x_2(0) \frac{\delta \epsilon(0)}{\epsilon_0(0)} = \delta y_1(0)x_2(0) + \delta y_3(0)x_4(0), \quad (26)$$

where  $\epsilon_0(0)$  is the value of the V/H ratio at the surface in the background medium. This equation is significant since it is equal to the left-hand side of eq. (24). Defining

$$J_{xy} = \int_{-\infty}^0 \frac{\partial F(\mathbf{x}, \mathbf{y})}{\partial k} dz \quad (27)$$

and making these substitutions in eq. (24) gives

$$y_1(0)x_2(0) \frac{\delta \epsilon(0)}{\epsilon_0(0)} = -\delta k J_{xy} - \int_{-\infty}^0 \frac{\partial F(\mathbf{x}, \mathbf{y})}{\partial \mu} \delta \mu dz. \quad (28)$$

Now, as in Tanimoto & Tsuboi (2009), we consider the case that the eigenfunctions are substituted in for the auxiliary functions. In this case, the left-hand side of eq. (28) is zero since  $y_2(0) = 0$ . Rearranging the right-hand side of eq. (28) gives a formula for the wavenumber perturbation:

$$\delta k = -\frac{1}{J_{yy}} \int_{-\infty}^0 \frac{\partial F(\mathbf{y}, \mathbf{y})}{\partial \mu} \delta \mu dz, \quad (29)$$

which is essentially an alternative expression for the phase velocity kernel. Returning to eq. (28), we can use eq. (29) to substitute for  $\delta k$  yielding

$$y_1(0)x_2(0) \frac{\delta \epsilon(0)}{\epsilon_0(0)} = \frac{J_{xy}}{J_{yy}} \int_{-\infty}^0 \frac{\partial F(\mathbf{y}, \mathbf{y})}{\partial \mu} \delta \mu dz - \int_{-\infty}^0 \frac{\partial F(\mathbf{x}, \mathbf{y})}{\partial \mu} \delta \mu dz. \quad (30)$$

Combining the two integrals' results in a perturbational expression for the ellipticity at the free-surface:

$$\delta \epsilon(0) = \frac{\epsilon_0(0)}{y_1(0)x_2(0)} \int_{-\infty}^0 \left[ \frac{J_{xy}}{J_{yy}} \frac{\partial F(\mathbf{y}, \mathbf{y})}{\partial \mu} - \frac{\partial F(\mathbf{x}, \mathbf{y})}{\partial \mu} \right] \delta \mu dz. \quad (31)$$

To obtain a non-perturbational approximation, we express the perturbations  $\delta \epsilon(0)$  and  $\delta \mu$  as their values  $\epsilon(0)$  and  $\mu$  minus their values in the homogeneous background medium  $\epsilon_0(0)$  and  $\mu_0$ :

$$\epsilon(0) - \epsilon_0(0) = \frac{\epsilon_0(0)}{y_1(0)x_2(0)} \int_{-\infty}^0 \left[ \frac{J_{xy}}{J_{yy}} \frac{\partial F(\mathbf{y}, \mathbf{y})}{\partial \mu} - \frac{\partial F(\mathbf{x}, \mathbf{y})}{\partial \mu} \right] \mu dz. \quad (32)$$

Note that  $\mu_0$  does not appear in this expression because

$$\int_{-\infty}^0 \left[ \frac{J_{xy}}{J_{yy}} \frac{\partial F(\mathbf{y}, \mathbf{y})}{\partial \mu} - \frac{\partial F(\mathbf{x}, \mathbf{y})}{\partial \mu} \right] dz = 0. \quad (33)$$

The fact that this integral is zero can be partially understood from the fact that the sensitivity kernel for ellipticity in depth is both positive and negative, in contrast to the phase velocity sensitivity kernel which is only positive. It turns out that the positive and negative portions are equal and the integral of the ellipticity sensitivity kernel over all depths evaluates to zero. Putting in the eigenfunctions and auxiliary functions for

a homogeneous medium into eq. (32) allows the analytical evaluation of the integrals through some involved algebraic manipulation. We do not show the details here and instead give the final result. Noting that density is taken to be constant [i.e.  $\mu(z) = \rho\beta^2(z)$ ], we obtain

$$\epsilon(0) = -1.4679 + \frac{1}{\beta_0^2(0)} \int_{-\infty}^0 \frac{\partial \tilde{g}(k, z)}{\partial z} \beta^2(z) dz, \quad (34)$$

where the kernel function  $\tilde{g}$  is given by

$$\tilde{g}(k, z) = -9.8819e^{1.6950kz} + 13.8923e^{1.2408kz} - 4.0103e^{0.7866kz}. \quad (35)$$

Note the presence of the squared shear wave velocity of the background medium at the surface in eq. (34). This comes from the shear modulus term in eq. (22) for the auxiliary function  $x_2$  in the background medium. However, the Dix approximation for Rayleigh waves assumes that the background medium  $\beta_0$  is homogeneous and changes at each frequency such that  $\beta_0 = c/0.9194$  for a Poisson medium, where  $c$  is the measured phase velocity at a particular frequency (Haney & Tsai 2015). Thus, at each frequency, the Earth is approximated as a different homogeneous medium with shear wave velocity  $\beta_0 = c/0.9194$ . This style of approximation is analogous to the Dix methodology in reflection seismology in which the subsurface above a reflector is approximated as a single homogeneous layer with a velocity given by the root-mean-square (RMS) velocity of the layers above the reflector. In that way, each reflector in the Earth is overlain by a different homogeneous medium. The same approximation for Rayleigh waves means that at each frequency a different homogeneous medium can be considered. Given this approximation, eq. (34) can be expressed in terms of the phase velocity

$$\epsilon(0) = -1.4679 + \frac{1}{c^2} \int_{-\infty}^0 \frac{\partial g(k, z)}{\partial z} \beta^2(z) dz, \quad (36)$$

where the kernel function  $g = 0.9194^2 \tilde{g}$  is given by

$$g(k, z) = -8.3532e^{1.6950kz} + 11.7432e^{1.2408kz} - 3.3899e^{0.7866kz}. \quad (37)$$

As can be seen from eq. (37),  $g(k, 0) = 0$  and  $g(k, -\infty) = 0$  and therefore for a homogeneous medium the integral in eq. (36) evaluates to zero.

An approximation for the H/V ratio (inverse of the V/H ratio) can be derived by recognizing that  $\delta\epsilon/\epsilon = -\delta\gamma/\gamma$ , since the quantities are inverses of each other. This leads to a similar expression for H/V ratio given by

$$\gamma(0) = -0.6812 + \frac{1}{c^2} \int_{-\infty}^0 \frac{\partial q(k, z)}{\partial z} \beta^2(z) dz, \quad (38)$$

where the kernel function  $q$  is given by

$$q(k, z) = 3.8767e^{1.6950kz} - 5.4500e^{1.2408kz} + 1.5733e^{0.7866kz}. \quad (39)$$

and it can be seen that  $q(k, z) = -g(k, z)/1.4679^2$ .

#### 4 MODELLING AND INVERSION

Eqs (36) and (38) suggest that there is a way to include ellipticity information in an approximate linear inversion procedure similar to Dix inversion encountered in reflection seismology. The connection between Dix inversion and surface wave phase velocity inversion has previously been shown by Haney & Tsai (2015). In that case, a linear relation exists for weakly heterogeneous layered media between squared shear wave velocity and squared phase velocity:

$$c^2(k) = \int_{-\infty}^0 \frac{\partial f(k, z)}{\partial z} \beta^2(z) dz, \quad (40)$$

where the kernel function  $f$  is given by

$$f(k, z) = 2.8454e^{1.6950kz} - 6.3096e^{1.2408kz} + 4.3095e^{0.7866kz}. \quad (41)$$

Note that there are sign changes in eq. (41) relative to the expressions shown in Haney & Tsai (2015) due to the  $z$ -axis being taken as positive upwards here. In the previous section, we have shown that a linear relation exists between squared shear wave velocity and squared phase velocity multiplied by the difference in the ellipticity from its value in a homogeneous medium (i.e.  $-1.4679$  for a Poisson medium). For the V/H ratio, this led in eq. (36) to the following linear integral relation between the product of squared phase velocity and differential ellipticity with squared shear velocity:

$$(\epsilon(0, k) + 1.4679) \times c^2(k) = \int_{-\infty}^0 \frac{\partial g(k, z)}{\partial z} \beta^2(z) dz. \quad (42)$$

Eqs (40) and (42) are independent and combining them yields a linear relation between squared shear wave velocity and the product of squared phase velocity and ellipticity itself, instead of differential ellipticity:

$$\epsilon(0, k) \times c^2(k) = \int_{-\infty}^0 \left( \frac{\partial g(k, z)}{\partial z} - 1.4679 \frac{\partial f(k, z)}{\partial z} \right) \beta^2(z) dz = \int_{-\infty}^0 \frac{\partial p(k, z)}{\partial z} \beta^2(z) dz, \quad (43)$$

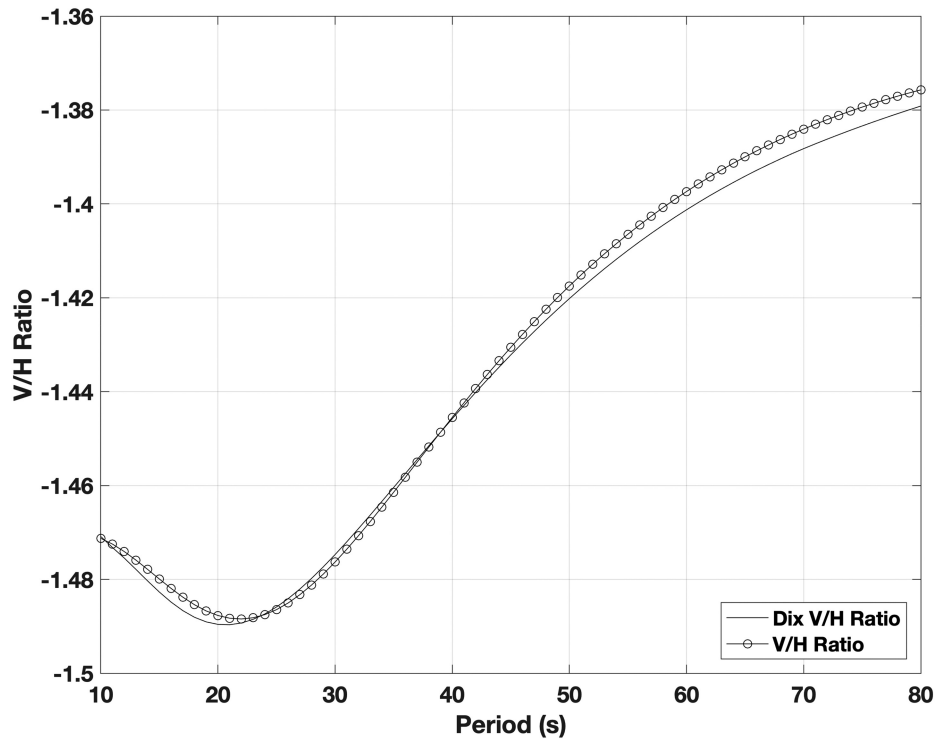


Figure 1. Comparison between approximate and true V/H ratios for the crustal-scale velocity model in Haney *et al.* (2020).

where the kernel  $p(k, z) = g(k, z) - 1.4679f(k, z)$  and is given by

$$p(k, z) = -12.5299e^{1.6950kz} + 21.0050e^{1.2408kz} - 9.7158e^{0.7866kz}. \tag{44}$$

Similarly for H/V ratio,

$$\gamma(0, k) \times c^2(k) = \int_{-\infty}^0 \left( \frac{\partial q(k, z)}{\partial z} - 0.6812 \frac{\partial f(k, z)}{\partial z} \right) \beta^2(z) dz = \int_{-\infty}^0 \frac{\partial b(k, z)}{\partial z} \beta^2(z) dz, \tag{45}$$

where the kernel  $b(k, z) = q(k, z) - 0.6812f(k, z)$  and is given by

$$b(k, z) = 1.9383e^{1.6950kz} - 1.1516e^{1.2408kz} - 1.3626e^{0.7866kz}. \tag{46}$$

Thus by eqs (43) and (45), a Dix-type inversion that includes ellipticity information exists for measurements that are the product of either V/H or H/V ratio with the squared phase velocity.

Shown in Fig. 1 is the approximation for V/H ratio in a crustal-scale velocity model from Haney *et al.* (2020) compared to the true values from full Rayleigh-wave modelling over the period band from 10 to 80 s. The crustal-scale model consists of a layer with a shear wave velocity of 3.8 km s<sup>-1</sup> and a thickness of 38 km overlaying a half-space with a shear wave velocity of 4.2 km s<sup>-1</sup>. Poisson’s ratio is fixed at 0.25. As can be seen in Fig. 1, the approximation is fairly good owing to the relatively weak velocity contrast between the layer and half-space. In the limit of a vanishingly weak contrast, the approximation converges to the true solution. The approximation is also applicable for periods shorter than 10 s, although those periods are not plotted in Fig. 1. In that case, the Rayleigh wave begins to only feel the upper layer and the behaviour approaches a homogeneous medium. This limiting value is captured by the first term in eq. (36) and therefore the integral in eq. (36) contributes progressively less and less as the period becomes shorter. Also of note in Fig. 1 is that a period exists for V/H ratio where the slope of the curve is zero, similar to the Airy phase in a group velocity dispersion curve. The exact period of the location of this zero slope in the V/H curve does not coincide with the Airy phase, but it has similar properties to the Airy phase in that it is related to the thickness of the layer. Similar features can be seen in crustal-scale V/H ratio plots shown in Chong *et al.* (2014).

We can represent the linear integral relation in eq. (40) in discrete form as

$$\vec{c}^2 = F \vec{\beta}^2, \tag{47}$$

and similarly for the relation in eq. (43)

$$\vec{\epsilon c}^2 = P \vec{\beta}^2, \tag{48}$$

where the matrices  $F$  and  $P$  are the discrete versions of the kernel functions  $f(k, z)$  and  $p(k, z)$  shown in eqs (41) and (44). For inversion of such matrix–vector relations between data and the squared shear wave velocity model, data covariance and model covariance matrices,  $C_d$

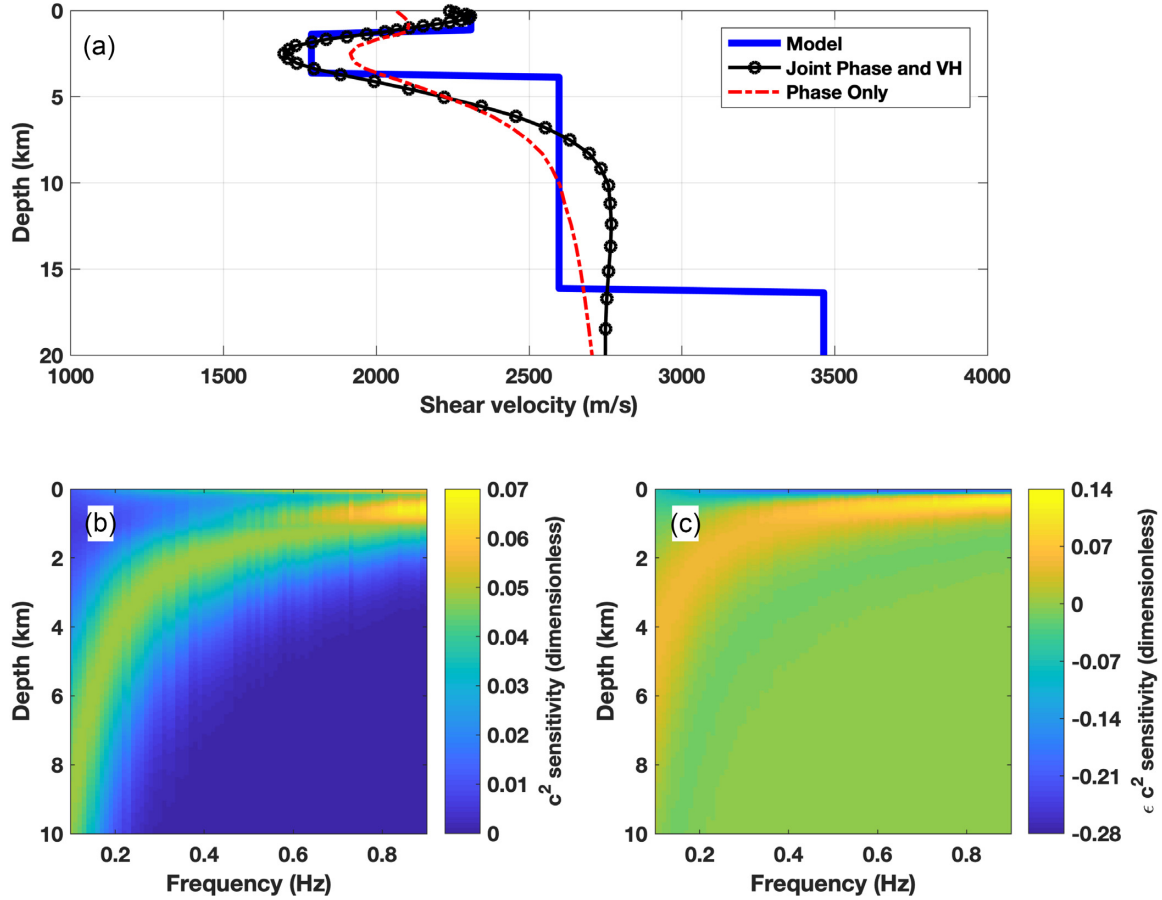


**Figure 2.** Test of the approximate V/H ratio expression within a linear Dix inversion scheme for shear wave velocity. (a) The joint inversion including both phase velocity and ellipticity information is observed to perform better than the inversion using only phase velocity. Panels (b) and (c) show the matrices  $F$  and  $P$  in eqs (47) and (48), which are the discrete versions of the kernel functions for squared phase velocity and the product of ellipticity and squared phase velocity. Note that panel (a) extends to 20 km depth, whereas panels (b) and (c) only plot to 10 km depth in order to show meaningful detail.

and  $C_m$ , are chosen as in Haney & Tsai (2017). The data covariance matrix is assumed to be a diagonal matrix:

$$C_d(i, i) = \sigma_d(i)^2, \quad (49)$$

where  $\sigma_d(i)$  is the data standard deviation of the  $i$ th measurement. The model covariance matrix has the form

$$C_m(i, j) = \sigma_m^2 \exp(-|z_i - z_j|/\ell), \quad (50)$$

where  $\sigma_m$  is the model standard deviation,  $z_i$  and  $z_j$  are the depths at the top of the  $i$ th and  $j$ th elements, and  $\ell$  is a smoothing distance or correlation length.

We note that when the data are squared phase velocity measurements, the data standard deviation  $\sigma_d$  has units of squared velocity. For a Rayleigh-wave velocity measurement given by  $c$  with standard deviation  $\sigma_c$ , the standard deviation of  $c^2$  is  $2c\sigma_c$ . If the data are instead the product of an ellipticity measurement (e.g. V/H ratio) and a squared phase velocity measurement, and the ellipticity measurement is given by  $\epsilon$  with standard deviation  $\sigma_\epsilon$ , then we compute the data standard deviation by using the propagation of errors formula and assuming the errors in the two measurements are uncorrelated. For example, if we denote the data as

$$d(\epsilon, c) = \epsilon c^2, \quad (51)$$

then its variance is given by

$$\sigma_d^2 = \left(\frac{\partial d}{\partial \epsilon}\right)^2 \sigma_\epsilon^2 + \left(\frac{\partial d}{\partial c}\right)^2 \sigma_c^2 = c^4 \sigma_\epsilon^2 + 4c^2 \epsilon^2 \sigma_c^2, \quad (52)$$

and this can be used for the data covariance matrix in eq. (49).

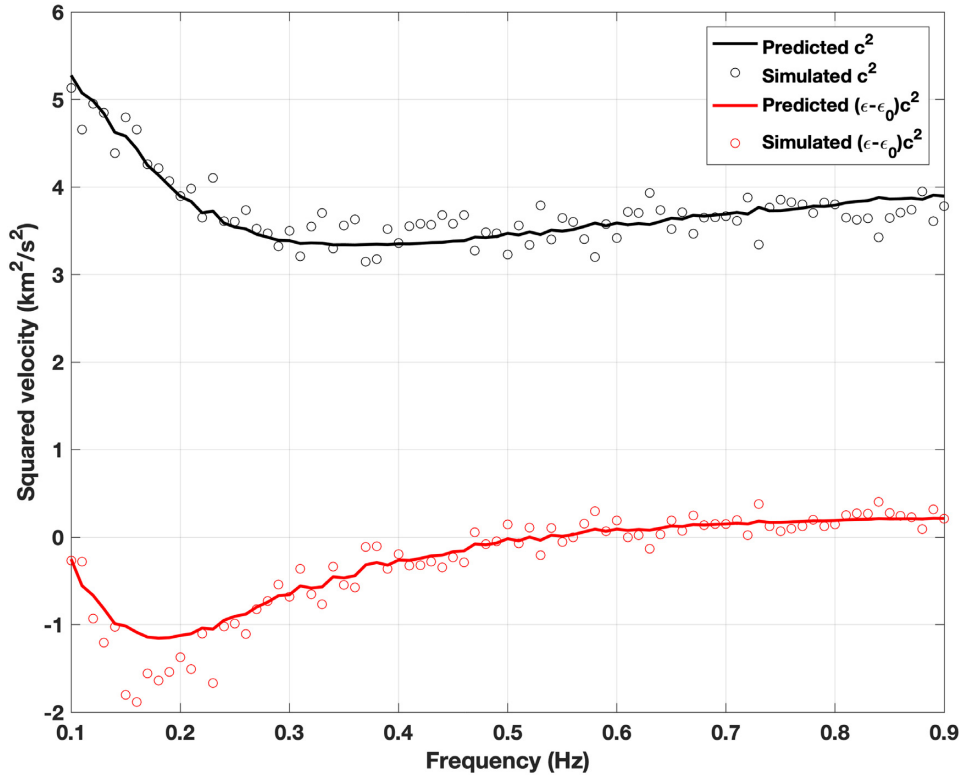


**Figure 3.** Data misfit for squared phase velocity and the product of differential V/H ratio and squared phase velocity for the joint inversion in Fig. 2. Differential V/H ratio is equal to  $\epsilon - \epsilon_0$ , where  $\epsilon$  is the V/H ratio and  $\epsilon_0$  is the V/H ratio in the homogeneous background medium ( $-1.4679$  for Poisson medium).

As shown in Haney & Tsai (2017), regularized Dix inversion of squared phase velocities can be posed as this augmented matrix system:

$$\begin{bmatrix} C_{c^2}^{-1/2} F \\ C_m^{-1/2} \end{bmatrix} \vec{\beta}^2 = \begin{bmatrix} C_{c^2}^{-1/2} \vec{c}^2 \\ C_m^{-1/2} \vec{\beta}_b^2 \end{bmatrix}, \tag{53}$$

where  $\beta_b$  is a background model intended to constrain  $\beta$  in regions with poor resolution (e.g., deeper than a wavelength below the surface). To include ellipticity information, we include another linear matrix–vector relation in the augmented matrix–vector system:

$$\begin{bmatrix} C_{c^2}^{-1/2} F \\ C_{\epsilon c^2}^{-1/2} P \\ C_m^{-1/2} \end{bmatrix} \vec{\beta}^2 = \begin{bmatrix} C_{c^2}^{-1/2} \vec{c}^2 \\ C_{\epsilon c^2}^{-1/2} \vec{\epsilon c}^2 \\ C_m^{-1/2} \vec{\beta}_b^2 \end{bmatrix}, \tag{54}$$

where now both  $c^2$  and  $\epsilon c^2$  are jointly inverted for a squared shear wave velocity model.

Shown in Fig. 2(a) are inversions based on the linear Dix method using both phase velocity and ellipticity (joint inversion) and only phase velocity. This is for the same example considered in Haney & Tsai (2017), with a low-velocity zone located below the surface and measurements of both phase velocity and ellipticity between 0.1 and 0.9 Hz. The Dix method using only phase velocities is seen to do fairly well and captures some indications of the low-velocity zone. However, the joint Dix inversion using both phase velocity and ellipticity information is observed to do much better, with a more accurate representation of the low-velocity zone and shear wave velocity values near the surface. In Figs 2(b) and (c), we plot the kernel matrices  $F$  and  $P$  that show the sensitivity for measurements of  $c^2$  and  $\epsilon c^2$ . The sensitivity of  $\epsilon c^2$  is overall shallower than  $c^2$  and also has a sign change in the upper 1 km of the subsurface. These characteristics yield improved sensitivity to structure in the upper 5 km for the joint inversion compared to the inversion of only phase velocity data. We note that, as in Haney & Tsai (2017), the synthetic data used for this example are corrupted with 2.5 per cent random noise. The matrices  $F$  and  $P$  are constructed from the noisy data through the dependence on  $k$  in eqs (41) and (44). Thus, the plots in Figs 2(b) and (c) show the effects of the noise as a small amount of roughness in the kernel matrices. Fig. 3 shows the data misfit for the joint inversion in terms of the squared phase velocity and the differential V/H ratio multiplied by the squared phase velocity. The predicted data from the joint inversion are observed to fit the synthetic data to within the noise, although some amount of misfit remains for the ellipticity data near 0.15 Hz. In addition, the presence of the 2.5 per cent random noise in this example can be observed in the predicted data as a small amount of roughness since the predicted data

are computed from the inverted model in Fig. 2(a) multiplied by the matrices  $F$  and  $P$ . This example demonstrates that ellipticity information can be included in such a non-perturbational methodology for inverting Rayleigh-wave data.

## 5 CONCLUSIONS

Using the generalized energy equation for Rayleigh waves, we have derived approximations for Rayleigh-wave ellipticity at the surface, in terms of either the V/H or H/V ratio, valid for weakly heterogeneous layered media. The results show that the product of ellipticity and squared phase velocity is linearly related to squared shear wave velocity in the subsurface and we have shown how such a relation can be used in a linear inversion scheme. A synthetic data example for a model with a low-velocity zone beneath the surface illustrates the joint inversion of phase velocity and ellipticity, which is shown to do better at shallow depths (relative to the wavelength) compared to inversion based on phase velocity only. Future topics to investigate include the analysis of density variations, expressions for power-law velocity profiles and the measurement of ellipticity at depth (i.e. not at the surface).

## ACKNOWLEDGEMENTS

We thank the editor, two anonymous reviewers and Roger Denlinger (U.S. Geological Survey, Cascades Volcano Observatory) for their perceptive and constructive comments. Any use of trade, firm or product names is for descriptive purposes only and does not imply endorsement by the U.S. Government.

## DATA AVAILABILITY

Only synthetic data were used in this paper and were produced with these previously published codes by Haney & Tsai (2017): [https://github.com/matt-haney/raylee\\_codes](https://github.com/matt-haney/raylee_codes). Specific scripts and modified versions of those codes used to make figures in this paper are available from the first author upon request by email.

## REFERENCES

- Ben-Menahem, A. & Singh, S.J., 1981. *Seismic Waves and Sources*, Springer-Verlag.
- Berg, E., Lin, F.-C., Allam, A.A., Qiu, H., Shen, W. & Ben-Zion, Y., 2018. Tomography of Southern California via Bayesian joint inversion of Rayleigh wave ellipticity and phase velocity from ambient noise cross-correlations, *J. Geophys. Res.*, **123**, 9933–9949.
- Boore, D. & Toksöz, M., 1969. Rayleigh wave particle motion and crustal structure, *Bull. Seism. Soc. Am.*, **59**, 331–346.
- Chieppa, D., Hobiger, M. & Fäh, D., 2020. Ambient vibration analysis on seismic arrays to investigate the properties of the upper crust: an example from Herdern in Switzerland, *Geophys. J. Int.*, **222**, 526–543.
- Chong, J., Ni, S. & Zhao, L., 2014. Joint inversion of crustal structure with the Rayleigh wave phase velocity dispersion and the ZH ratio, *Pure Appl. Geophys.*, **172**, 2585–2600.
- Dix, C.H., 1955. Seismic velocities from surface measurements, *Geophysics*, **20**, 68–86.
- Ewing, W.M., Jardetsky, W.S. & Press, F., 1957. *Elastic Waves in Layered Media*, McGraw-Hill.
- Fäh, D., Kind, F. & Giardini, D., 2001. A theoretical investigation of average H/V ratios, *Geophys. J. Int.*, **145**, 535–549.
- Fäh, D., Kind, F. & Giardini, D., 2003. Inversion of local S-wave velocity structures from average H/V ratios, and their use for the estimation of site-effects, *J. Seismol.*, **7**, 449–467.
- Haney, M.M. & Tsai, V.C., 2015. Nonperturbational surface wave inversion: a Dix-type relation for surface waves, *Geophysics*, **80**, EN167–EN177.
- Haney, M.M. & Tsai, V.C., 2017. Perturbational and nonperturbational inversion of Rayleigh waves, *Geophysics*, **82**, F15–F28.
- Haney, M.M., Ward, K.M., Tsai, V.C. & Schmandt, B., 2020. Bulk structure of the crust and upper mantle beneath Alaska from an approximate Rayleigh-wave dispersion formula, *Seismol. Res. Lett.*, **91**, 3064–3075.
- Hobiger, M. *et al.*, 2013. Ground structure imaging by inversions of Rayleigh wave ellipticity: sensitivity analysis and application to European strong motion sites, *Geophys. J. Int.*, **192**, 201–229.
- Jeffreys, H., 1935. The surface waves of earthquakes, *Mon. Not. Roy. Astron. Soc. Geophys. Suppl.*, **3**, 253–261.
- Lin, F.-C., Tsai, V.C. & Schmandt, B., 2014. 3-D crustal structure of the western United states: application of Rayleigh-wave ellipticity extracted from noise cross-correlations, *Geophys. J. Int.*, **198**, 656–670.
- Malischewsky, P.G. & Scherbaum, D., 2004. Love's formula and H/V-ratio (ellipticity) of Rayleigh waves, *Wave Motion*, **40**, 57–67.
- Maupin, V., 2017. 3-D sensitivity kernels of the Rayleigh wave ellipticity, *Geophys. J. Int.*, **211**, 107–119.
- Meyers, P., Bowden, D.C., Prestegard, T., Tsai, V.C., Mandic, V., Pavlis, G. & Caton, R., 2019. Direct observations of surface-wave eigenfunctions at the homestake 3D array, *Bull. Seism. Soc. Am.*, **109**, 1194–1202.
- Muir, J.B. & Tsai, V.C., 2017. Rayleigh wave H/V via noise cross-correlation in southern California, *Bull. Seism. Soc. Am.*, **107**, 2021–2027.
- Tanimoto, T. & Alvizuri, C., 2006. Inversion of the HZ ratio of microseisms for S-wave velocity, *Geophys. J. Int.*, **165**, 323–335.
- Tanimoto, T. & Tsuboi, S., 2009. Variational principle for Rayleigh wave ellipticity, *Geophys. J. Int.*, **179**, 1658–1668.
- Tsuboi, S. & Saito, M., 1983. Partial derivatives of Rayleigh wave particle motion, *J. Phys. Earth*, **31**, 103–113.

## APPENDIX A: RESULTS FOR GENERAL VALUES OF POISSON'S RATIO

Here we give expressions for phase velocity and ellipticity valid in the weak heterogeneity limit, which depend on Poisson's ratio, in contrast to the equations shown in the main text that were specific to a Poisson's ratio of 0.25. To make the notation most efficient, we use these parameters:

$$r = \frac{\lambda}{\mu}, \tag{A1}$$

and

$$t(r) = \frac{c^2(r)}{\beta^2}, \quad (\text{A2})$$

where  $r$  is the ratio of the elastic moduli and  $t$  is the ratio of the squared Rayleigh-wave phase velocity to the squared shear wave velocity of a homogeneous half-space. Poisson's ratio  $\sigma$  is expressible in terms of  $r$  as  $\sigma(r) = r/(2 + 2r)$ . For a Poisson medium,  $r = 1$  and  $\sqrt{t} = 0.9194$ . The ratio  $t$  is a complicated function of  $r$ , but for completeness we show it here as

$$t(r) = \frac{8}{3} + \frac{4(r-4)}{3w(r)} - \frac{2w(r)}{3(2+r)}, \quad (\text{A3})$$

where

$$w(r) = (1+r) \left( \frac{28r^3}{(1+r)^3} - \frac{123r^2}{(1+r)^2} + \frac{156r}{(1+r)} - 44 + \frac{3\sqrt{3}}{(1+r)^3} \sqrt{(2+r)^3(11r^3 + 4r^2 - 9r - 10)} \right)^{\frac{1}{3}}. \quad (\text{A4})$$

We further simplify the notation by using these functions of  $r$  and  $t(r)$ :

$$u(r) = \sqrt{1 - \frac{t(r)}{r+2}}, \quad (\text{A5})$$

and

$$v(r) = \sqrt{1 - t(r)}. \quad (\text{A6})$$

With these functions  $u$  and  $v$ , the Rayleigh eigenfunctions for general Poisson's ratio are given by

$$\hat{y}_3(k, z, u, v) = e^{ukz} - \left( \frac{1+v^2}{2} \right) e^{vkz}, \quad (\text{A7})$$

and

$$\hat{y}_1(k, z, u, v) = ue^{ukz} - \left( \frac{1+v^2}{2v} \right) e^{vkz}. \quad (\text{A8})$$

By working through the procedure shown in Haney & Tsai (2015) with these eigenfunctions for general Poisson's ratio, we find this expression for the phase velocity kernel function  $\hat{f}$  valid for all values of Poisson's ratio:

$$\hat{f}(k, z, u, v) = \frac{f_1(u, v)e^{2ukz} - f_2(u, v)e^{(u+v)kz} + f_3(u, v)e^{2vkz}}{u - 5uv^2 + 4(1+u^2)v^3 - 5uv^4 + uv^6}, \quad (\text{A9})$$

where the functions  $f_1, f_2$  and  $f_3$  are given by

$$f_1(u, v) = 4v^3(1 - v^2 + u^2(7 + v^2)), \quad (\text{A10})$$

$$f_2(u, v) = 16uv^2(1 + uv)(1 + v^2), \quad (\text{A11})$$

$$f_3(u, v) = u(1 + v^2)^2(1 + 6v^2 + v^4). \quad (\text{A12})$$

Note that the kernel function  $f(k, z)$  given in the main text by eq. (41) is equal to  $\hat{f}$  when  $r = 1$ , which is the case of a Poisson medium with a Poisson's ratio of 0.25. Although the expression in eq. (A9) is more complicated than eq. (41), it maintains the property of being the sum of three exponentials that are functions of depth.

Moving on to ellipticity, using the eigenfunctions in eqs (A7) and (A8) in the same procedure as discussed in the main text leads to

$$\hat{g}(k, z, u, v) = \frac{g_1(u, v)e^{2ukz} + g_2(u, v)e^{(u+v)kz} - g_3(u, v)e^{2vkz}}{2v(1-v^2)(u(7v^4 + 6v^2 - 1) - 4(1+2u^2))}, \quad (\text{A13})$$

where the functions  $g_1, g_2$  and  $g_3$  are given by

$$g_1(u, v) = 2v(1 - v^2 + u^2(7 + v^2))(1 + v^2(5v^2 - 4uv - 2)), \quad (\text{A14})$$

$$g_2(u, v) = 4(1 + uv)(4v^3 + 16u^2v^3 - 4v^5 - u(1 + v^2)^2(1 + 3v^2)), \quad (\text{A15})$$

$$g_3(u, v) = (1 + 7v^2 + 7v^4 + v^6)(2v - 2v^3 - 2u^2v(v^2 - 3) + u(v^2 - 3)(1 + v^2)). \quad (\text{A16})$$

Finally note that the kernel function  $g(k, z)$  given in the main text by eq. (37) is equal to  $\hat{g}$  when  $r = 1$  as it should. Eq. (A13) also maintains the property of being the sum of three exponentials that are functions of depth as seen previously for phase velocity. From these expressions for  $\hat{f}$  and  $\hat{g}$ , similar expressions for  $\hat{q}$ ,  $\hat{p}$  and  $\hat{b}$  can be constructed as generalizations of eqs (39), (44) and (46) valid for any Poisson's ratio.

This requires the following general relation for V/H ratio at the surface of a homogeneous half-space (Malischewsky & Scherbaum 2004):

$$\hat{\epsilon}(0, r) = \frac{t(r) - 2}{2\sqrt{1 - t(r)}}, \quad (\text{A17})$$

where we note the sign change compared to the expression in Malischewsky & Scherbaum (2004) since that expression is for the absolute value of the V/H ratio. The equations for  $\hat{q}$ ,  $\hat{p}$  and  $\hat{b}$  follow as

$$\hat{q}(k, z, u, v) = -\frac{\hat{g}(k, z, u, v)}{\hat{\epsilon}^2(0, r)} \quad (\text{A18})$$

$$\hat{p}(k, z, u, v) = \hat{g}(k, z, u, v) + \hat{\epsilon}(0, r)\hat{f}(k, z, u, v) \quad (\text{A19})$$

$$\hat{b}(k, z, u, v) = \hat{q}(k, z, u, v) + \frac{\hat{f}(k, z, u, v)}{\hat{\epsilon}(0, r)}. \quad (\text{A20})$$